Ryabov, B. I.; Bezrukov, D. A.; Kallunki, J.

Low Brightness Temperature in Microwaves at Periphery of Some Solar Active Regions

Published in:
Latvian Journal of Physics and Technical Sciences

DOI:
10.1515/lpts-2017-0021
10.1515/lpts-2017-0021

Published: 27/06/2017

Document Version
Publisher's PDF, also known as Version of record

LATVIAN JOURNAL OF PHYSICS AND TECHNICAL SCIENCES
2017, N 3

DOI: 10.1515/lpts-2017-0021

ASTROPHYSICS

LOW BRIGHTNESS TEMPERATURE IN MICROWAVES AT PERIPHERY OF SOME SOLAR ACTIVE REGIONS

B. I. Ryabov[1], D. A. Bezrukov[1], J. Kallunki[2]
[1] Ventspils International Radio-Astronomy Centre,
101 Inzenieru Str., Ventspils, LV- 3601, LATVIA
e-mail: virac@venta.lv
[2] Aalto University Metsähovi Radio Observatory,
Metsähovintie 114, FIN-02540 Kylmälä, Finland

The microwave regions with low brightness temperature are found to overlap the regions of the depressed coronal emission and open field lines at the periphery of two solar active regions (ARs). The imaging microwave observations of the Sun with the Nobeyama Radio heliograph at 1.76 cm, the MRO-14 radio telescope of Metsähovi Radio Observatory at 0.8 cm, and the RT-32 of Ventspils International Radio Astronomy Centre in the range 3.2–4.7 cm are used. To reduce the noise in the intensity distribution of the RT-32 maps of the Sun, one wavelet plane of "*à trous*" wavelet space decomposition is subtracted from each map. To locate the open-field regions, the full-Sun coronal magnetic fields with the potential field source surface (PFSS) model for $R_{SS} = 1.8\ R_\odot$ are simulated. We conclude that the revealed LTRs present narrow coronal hole-like regions near two ARs and imply an extra investigation on the plasma outflow.

Keywords: *microwave radiation, solar atmosphere, solar active region*

1. INTRODUCTION

An attempt to restore the low-contrast microwave structures on the maps of the Sun, which were scanned with the Ventspils International Radio-Astronomy Center RT-32 radio telescope, was undertaken in [1]. In 2012, a new multichannel spectral polarimeter was installed on the 32-meter antenna [2], and a number of observations were performed in 2013–2014. In 2016, solar observations were renewed after major reconstruction of the RT-32 radio telescope. The spectral polarimeter was significantly improved. Nevertheless, the problem of the recovery of the low-contrast sources is still present.

Here, we attempt to make more discernible the regions with low brightness temperature on the RT-32 maps. We use the wavelet transform to decompose each map into a smoothed map and three wavelet planes. To reduce the noise, the noisiest wavelet plane is subtracted from the map. To evaluate the corresponding modifications, we compare the resulted RT-32 maps with the microwave maps obtained with the Nobeyama Radio heliograph (NoRH) and the 14-meter dish of the Metsähovi Radio Observatory (MRO-14) under higher resolution and well-formed diagram pattern.

At the MRO [3], the low-brightness-temperature regions (LTRs) are investigated longer than two solar cycles [4]. It has been established that two thirds of the compact LTRs at the wavelength of 0.8 cm are associated with the dark Hα filaments [5] and the neutral line (NL) of the longitudinal component of the magnetic field.

Two compact LTRs, which are close to a solar active region (AR) but apart from the NL, are analysed in the present research. We investigate if these LTRs are associated with the coronal partings (CPs; [6]) or, in terms of [7], coronal hole-like structures near ARs. Some authors (see [7], [8] for the reviews) have noted that the region of depressed coronal emission and open magnetic field lines at the edges of some ARs indicates the local source of the nascent slow solar wind. In some cases, the depressed soft X-ray coronal emission is accompanied by the depressed microwave emission at the periphery of the isolated sunspots [9], [10].

To simulate the open magnetic field lines, we make use of the Potential Field Source Surface (PFSS) model [11], [12]. However, we adopt the values of the free model parameter that is less than the usual one, $R_{SS} = 2.5\ R_{\odot}$, where $R_{\odot}$ denotes the radius of the Sun.

Section 2 briefly describes the wavelet decomposition of the RT-32 map in 2D space and the noise suppression in the map. Two examples of the LTRs are analysed in Section 3. In Section 4, we discuss the evidence for the open magnetic field lines above the two areas of the depressed coronal (soft X-ray and EUV) emission as well as microwave emission near the associated ARs. We conclude that the microwave observations of the LTRs have potential for determining the coronal hole-like structures near ARs.

2. DATA REDUCTION

2.1 RT-32 Diagram Pattern

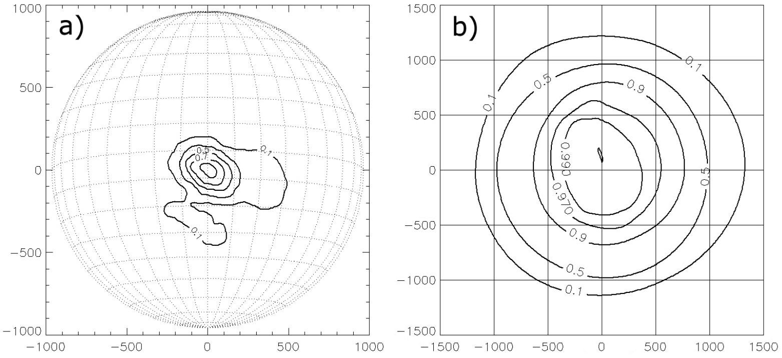

Fig. 1. The position of the RT-32 diagram pattern and model quiet Sun at the wavelength 3.2 cm on 18 March 2014. (a) The point source *Cyg* A scanned with the help of the radio telescope RT-32. (b) Brightness distribution of the model quiet Sun: the disk of the uniform radio brightness, $R = 1.026\ R_{\odot}$, convolved with the diagram pattern of the RT-32. Hereinafter the axes denote seconds of arc from the centre of the solar disk.

It should be noted that the positioning of the RT-32 diagram pattern was revised (Fig. 1a) since the results of [1]. The RT-32 with the solar spectral polarimeter makes available 16 maps in each Stokes I and V per session of scanning [13]. The 16 operational wavelengths lie in the range of 3.2–4.7 cm; the HPBWs are of 3.′4–5.′0.

2.2 Wavelet Transform and Noise Reduction

To proceed with the wavelet transform, the RT-32 microwave maps of the Sun are considered as some diffuse, noisy, and more or less isotropic images with discontinuities at the edges (solar limbs; Fig. 2a). We make use of the "*a trous"* ("with holes") non-orthogonal isotropic wavelet transform [14] for the approximation and de-noising of the image (Fig. 2.b). The decomposition of the image in 2D space domain consists of only three wavelet planes plus the smoothed image (Fig. 3).

The observed intensities are considered as the scalar product with scaling function, which corresponds to a low-pass filter presented by the B-spline of degree three [13]. The original 2D image is decomposed by means of row-by-row convolution with 1D filter followed by column-by-column convolution relying on separability [14]. Finally, the decomposition consists of the smoothed image (Fig. 3a) and three wavelet planes (Fig. 3b-d) of the same dimension as the initial image, while the distance between the adjacent pixels increases as 2^i [14].

To reduce noise, we subtract the first wavelet plane, i = 1, with finest scale of space signatures (Fig. 3d) from decomposition [16]. The result is shown in Fig.–s 2b and 4a. The evidential reasoning for the subtraction is the following: (a) this wavelet plane is the noisiest; (b) it contains the fluctuations due to time varying background; (c) the subtraction reveals some fine reliable structures; (d) the flux over this wavelet plane does not exceed 3 % of the total radio flux. After subtraction, the total radio flux is corrected to the initial level.

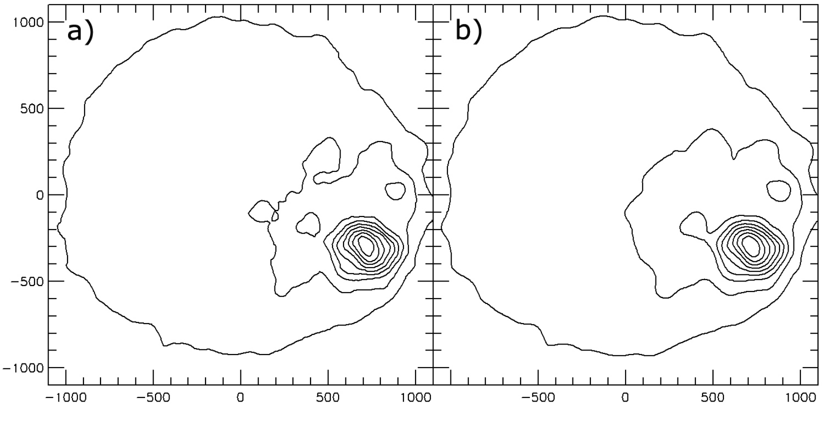

Fig. 2. Radio image of the Sun at 3.41 cm taken with the RT-32 on 16 May 2012: (a) dirty and (b) cleaned image. The image (b) resulted from the subtraction of the third wavelet plane (Fig. 3d) from the image (a).

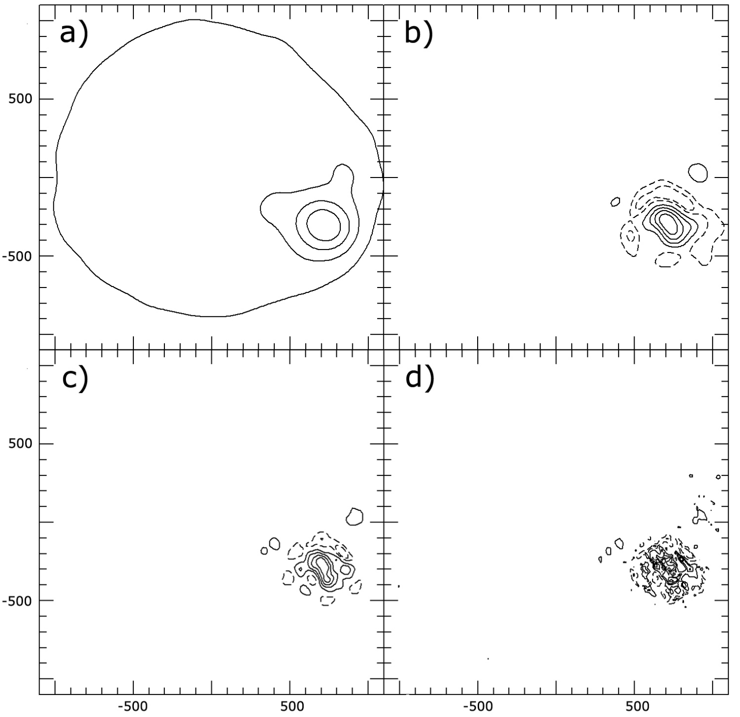

Fig. 3. The spatial decomposition of the radio image in Fig. 2a by "*à trous"* wavelet transform. The smoothed image (a) and three wavelet planes of the alternating-sign intensity (b-d) make up the image. The wavelet plane (d) with the lowest signal-to-noise ratio and the total flux < 3 % of the image is taken to be the noise and removed from the image.

3. LOW BRIGHTNESS TEMPERATURE REGIONS

The model simulations [17] show that the predominant part of the free-free radiation at mm wavelengths comes from the chromospheric layers. Nevertheless, let us compare the position of the LTRs with the position of the coronal hole-like structures [7] or, in other terms, the coronal partings [6]. The premise underlying such a comparison is some vertical magnetic structure, which implicates all the layers of the solar atmosphere. The indications of this joint structure are the following. (1) The reduced brightness temperature is observed not only at short cm but also at 6.6 cm, for the radiation from higher atmospheric layers [17]. (2) With the help of the chromospheric magnetogram, the CPs can be traced to the line dividing two magnetic arcades [6]. (3) The dark lane associated with the CP can be observed not only in the coronal emission but also in the chromospheric lines Hα and He 10830Å [6]. (4) The open magnetic field lines simulated with the PFSS model under Rss= 1.8 $R_\odot$ overlap with the dark lane of both the coronal and the short cm emission [10].

In the following subsections, the estimates of the LTR intensity are related to the brightness temperature of the quiet Sun, T^{qS}, which is taken as the following: 10^4 K at 1.76 cm [19], 8200 K at 0.8 cm [20], and 12.3 10^3 K at 3.2 cm [21]. We compare radio images with the longitudinal magnetograms from the Solar and Heliospheric

Observatory, Michelson Doppler Imager (SOHO MDI), soft X-ray images from the Hinode X-ray Telescope (Hinode XRT), and the extreme ultraviolet (EUV) images from the Solar Dynamics Observatory, Atmospheric Imaging Assembly (SDO AIA).

3.1 Active Region 11520

The arrows in Fig. 4 and Fig. 6a point to the LTR at the periphery of the AR 11520. The RT-32 main beam of the size Θ = 3′.6 smoothes a scarcely discernible depression at 3.41 cm. The LTR intensity is reduced by ~ 2 % relative to the quiet Sun level at 0.8 cm (Θ = 2.′4) and 1.76 cm (Θ = 0.′2).

The simulations by means of the PFSS model resulted in an open-field region overlying the LTR (Fig. 4c). Note that the magnetic polarity between the coronal hole CH 523 (Fig. 6a) and the region of the LTR (Fig. 4d) all the way is the same except a few small patches of the opposite polarity.

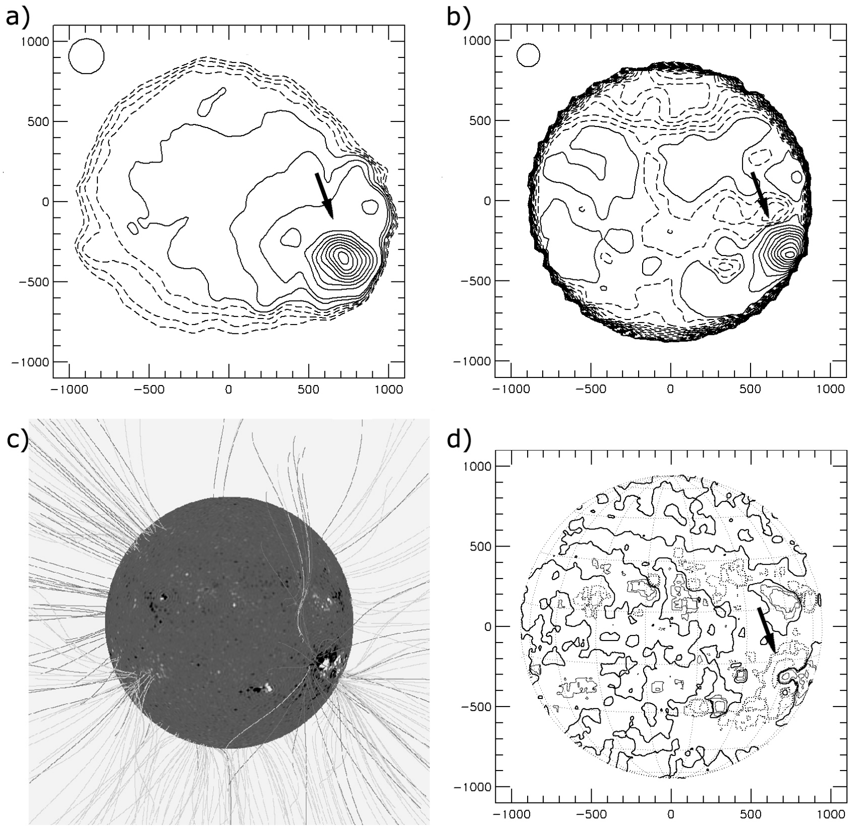

Fig. 4. Sun on 16 July 2012: (a) radio map at 3.41 cm taken with the VIRAC RT-32 at 13:19 UT; (b) radio map at 0.8 cm taken with the MRO-14 at 06:56 UT; (c) open magnetic field lines; and (d) longitudinal magnetogram taken with the SOHO MDI at 12:58 UT. Here and in the next figure, the levels of the brightness temperature of the LTRs (dashed lines on the panels (a) and (b)) are below the quiet Sun level, T^{qS}, with the step of 5 10^{-2} T^{qS} at cm wavelengths and of 5 10^{-3} T^{qS} at 8 mm. The neutral lines (solid curves on the panel (d)) separate the isolines of opposite magnetic polarity at ± (5, 10, 50, and 200) G. The arrow points to the location of the LTR as seen at the wavelength of 0.8 cm. It is assumed to be a coronal hole-like structure in the open magnetic field lines near the AR 11520 (see the text).

3.2 Active Region 11793

The arrows in Fig. 5 point to the LTR at the periphery of the AR 11793. Under the high spatial resolution of the NoRH, the LTR looks like the extension from the large CH 575 towards the AR 11793 (Fig. 6b). This linkage is a hint of similar nature of this LTR and the CH. Indeed, the simulated field lines are open just over the LTR.

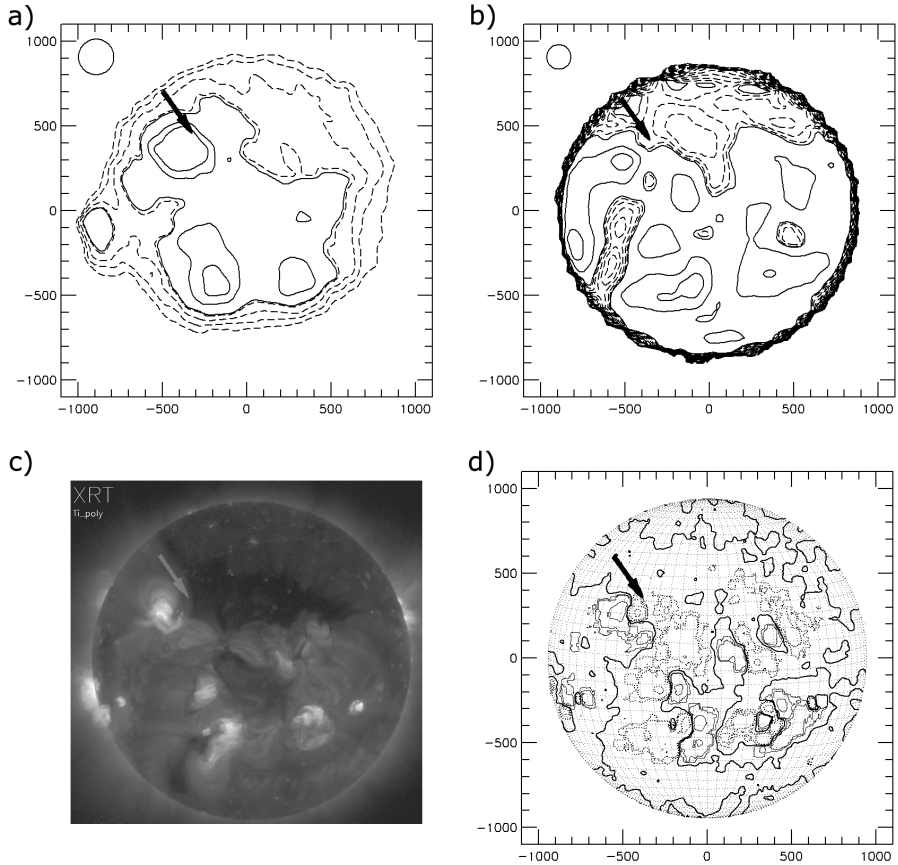

Fig. 5. Sun on 18 July 2013: (a) radio map at 3.26 cm taken with the VIRAC RT-32 at 11:45 UT; (b) radio map at 0.8 cm taken with the MRO-14 at 11:30 UT; (c) soft X-ray image taken with the Hinode XRT at 06:36 UT; and (d) longitudinal magnetogram taken with the SOHO MDI at 10:58 UT. The arrow goes along the location of the coronal hole-like structure as seen as reduced soft X-ray emission and the LTR at 0.8 cm in the open magnetic field lines near the AR 11793.

The magnetic polarity between the CH 575 and the region of the LTR (Fig. 5d) all the way is the same. The soft X-ray emission above the microwave LTR is not as much reduced as the emission in the neighbouring CH. It may be the projection affect: some bright coronal loops overlap with the LTR when not far from the eastern solar limb.

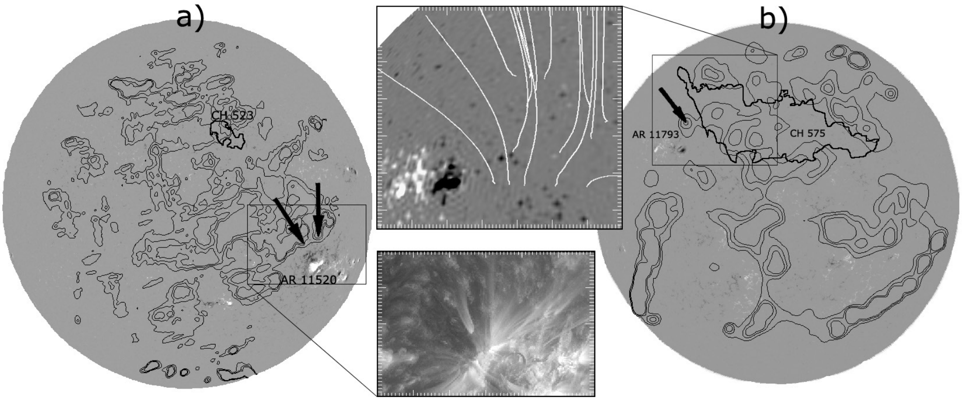

Fig. 6. The contours of the LTRs at the wavelength 1.76 cm overlaid on the Hinode HMI magnetogram. The observations are performed on (a) 16 July 2012 and (b) 18 July 2013 (the near-limb part of both HMI magnetograms is deleted). The NoRH 1.76 cm intensity radio map contours are at levels (0.98, 0.99, and 1.02) T^{qS}. The bold black line delineates the CHs (courtesy of the Solar Terrestrial Activity Reports). The arrow points to the LTR at the periphery of the corresponding active region. The cut–out from the global image (a) shows a close–up of the AR 11520 in Fe IX EUV line (SDO Atmospheric Imaging Assembly 171 Å). The cut–out from the global image (b) shows a close–up of the AR 11793 as HMI magnetogram with simulated open field lines.

Note, the two directions of the LTRs (two arrows in Fig. 6a) trace two coronal partings as well. More eastern CP goes towards the CH 523.

4. DISCUSSION AND CONCLUSIONS

We have presented two microwave LTRs, each associated with the depressed coronal emission and the open-field region at the periphery of two ARs (that is a coronal hole-like structure by the convention in [7]). This finding specifies the list of the LTRs and poses the problem of the analysis of the prospective sources of slow solar wind. The tasks of such an analysis (see, for example, [22]) are out of scope of the present research. Let us only note that the best-fit values for the free model parameter in the PFSS simulations of the open field lines near an AR are in the range R_{SS} = 1.6-1.8 $R_{\odot}$.

The higher the spatial resolution of microwave observation is, the more confident the association of LTR with the coronal hole-like structure is. The LTRs at 1.76 cm near the AR 11520 are associated with the coronal hole-like structure. With an order of magnitude lower spatial resolution at 0.8 cm, the only LTR has been found near the AR 11520. As for the maps taken with resolution of 3′–4′ in the wavelength range 3.2–4.7 cm, there is not any continuous modification of the reduced intensity of the LTRs from one wavelength to another. In addition to the not-completely-restored structures of the LTRs, there is some complicated gyro-resonance contribution to the intensity in cm wavelengths [23]. The bright gyro-resonance emission conceals the depressed emission near the cores of the sunspot-associated microwave sources.

Our conclusions are as follows:

1. The noise reduction in the RT-32 maps by means of "*a trous*" wavelet decomposition is useful, since it makes clearer the low-contrast structures.
2. The comparison of the RT-32 maps taken in the wavelength range 3.2–4.7 cm (HPBW = 3′–4′) with the NoRH maps at 1.76 cm (0.′12) and the MRO-14 maps at 0.8 cm (2.′4) shows a specific LTR at the periphery of two large ARs. The characteristic depression of the intensity is estimated to be of ~2 % at the wavelengths of 0.8 cm and 1.76 cm.
3. The LTR near ARs has the following features: (a) the depressed coronal (X-ray and EUV) emission and (b) open-field region simulated with the PFSS under R_{SS} = 1.8 $R_{\odot}$. These features present the coronal hole-like structure [7].

The detection of the LTR in line with the coronal hole-like structure stimulates further investigations to locate the sources of slow solar wind [10]. The procedures for such investigations are well elaborated for peripheral areas of ARs [22], [24], [25]. We will apply them in further research.

ACKNOWLEDGEMENTS

The research has been supported by the Latvian Ministry of Education and Science within the framework of the programme "Next Generation Information and Communication Technologies".

REFERENCES

1. Bezrukov, D.A., Ryabov, B.I., Zalite, K., & Bajkova, A.T. (2009). Application of recovering procedures to RT-32 radio maps of the Sun. *Latv. J. Phys. Tech. Sci., 6*, 49–56.
2. Bezrukov, D. (2013). Spectral polarimatric observations of the Sun by the VIRAC RT-32 radio telescope: First results. *Baltic Astronomy*, *22*, 9–14.
3. Kallunki, J., Lavonen, N., Järvelä, E., & Uunila, M. (2012). A study of long-term solar activity at 37 GHz. *Baltic Astronomy*, *21*, 255–262.
4. Brajša, R., Vršnak, B., Ruždjak, V., Jurač, S., Pohjolainen, S., Urpo, H., & Teräsranta, H. (1992). Giant cells on the Sun revealed by low temperature microwave regions? *Hvar Obs. Bull*., *16*, 1, 1–12.
5. Brajša, R., Ruždjak, V., Vršnak, B., Wöhl, H., Pohjolainen, S., & Urpo, H. (1999). An estimate of microwave low-brightness-temperature regions' heights obtained measuring their rotation velocity. *Solar Physics*, *184*, 281–296.
6. Nikulin, I.F. & Dumin, Y.V. (2016). Coronal partings. *Advances in Space Research,* 57(3), 904–911.
7. Brooks, D., Ugarte-Urra, I., & Warren, H.P. (2015). Full-Sun observations for identifying the sources of the slow solar wind. *Nature Communications*, *6*, 5947.
8. Poletto, G. (2013). Sources of solar wind over the solar activity cycle. *Journal of Advanced Research*, *4*, 215–220.

9. Ryabov, B.I., Gary, D.E., Peterova, N.G., Shibasaki, K., & Topchilo, N.A. (2015). Reduced coronal emission above large isolated sunspots. *Solar Physics*, *290*, 21–35. DOI:
10. Ryabov, B.I. & Shibasaki, K. (2016). Depressed emission between magnetic arcades near a sunspot. *Baltic Astronomy*, *25*, 225–235.
11. Schatten K. H., Wilcox J. M., & Ness N. F. (1969). A model of interplanetary and coronal magnetic fields. *Solar Physics*, *6*, 442–455.
12. Schrijver, C. J., DeRosa, M. L., & Title, A. M. (2010). Magnetic field topology and the thermal structure of the corona over solar active regions. *ApJ*, *719*, 1083–1096.
13. Bezrukov, D. (2013). Spectral polarimetric observations of the Sun by the VIRAC RT-32 radio telescope: First results. *Baltic Astronomy*, *22*, 9–14.
14. Starck, J.-L. & Murtagh, F. (1994). Image restoration with noise suppression using the wavelet transform. *Astron. Astrophys.*, *288*, 342–348.
15. Starck, J.-L., Murtagh, F., & Bertero, M. (2011). Starlet transform in astronomical data processing. In O. Scherzer (Ed.), *Handbook of Mathematical Methods in Imaging* (pp. 1489–1531). Springer.
16. Stenborg, G. & Cobelli, P.J. (2003). A wavelet packets equalization technique to reveal the multiple spatial-scale nature of coronal structures. *A&A*, *398*, 1185–1193.
17. Wedemeyer, S., Bastian, T., Brajša, R., Hudson, H., Fleishman, G., Loukitcheva, M., Barta, M. (2016). Solar science with the Atacama large millimeter/submillimeter array–a new view of our Sun. *Space Sci. Rev*., *200*, 1–73.
18. Brosius, J.W. & White, S.M. (2004). Close association of an extreme-ultraviolet sunspot plume depressions in the sunspot radio emission. *Ap. J., 601*, 546–558.
19. Koshiishi, H. (2003). Restoration of solar images by the Steer algorithm. *Astron. Astrophys*. *412*, 893–896.
20. Landi, E. & Chiuderi Drago, F. (2008). The quiet-Sun differential emission measure from radio and UV measurements. *Ap. J., 675*, 1629–1636.
21. Borovik, V.N., Kurbanov, M.S., & Makarov, V.V. (1992). Distribution of radio brightness of the quiet Sun in the 2-32 cm range. *Astron. J., 69*, 1288–1302.
22. Slemzin V., Harra L., Urnov A., Kuzin S., Goryaev F., & Bergman D. (2013). Signatures of the slow solar wind streams from active regions in the inner corona. *Solar Physics*, *286*, 157–184.
23. Bezrukov, D., Ryabov, B., Peterova, N., & Topchilo, N. (2011). Sharp changes in the ordinary mode microwave emission from a stable sunspot: Model analysis. *Latv. J. Phys. Tech. Sci., 48*(2), 56–69.
24. Liewer, P.C., Neugebauer, M., & Zurbuchen, T. (2004). Characteristics of active-region sources of solar wind near solar maximum. *Solar Physics*, *223*, 209–229.
25. Baker, D., van Driel-Gesztelyi, L., Mandrini, C. H., Démoulin, P., & Murray, M. J. (2009). Magnetic reconnection along quasi-separatrix layers as a driver of ubiquitous active region outflows. *Ap. J.*, *705*, 926–935.

SAMĒRĀ MAZA MIKROVIĻŅU EMISIJAS SPOŽUMA TEMPERATŪRA PIE SAULES AKTĪVIEM APGABALIEM

B. Rjabovs, D. Bezrukovs, J. Kallunki

K o p s a v i l k u m s

Divu Saules aktīvo apgabalu perifērijā atrasti divi mikroviļņos ar zemu spožuma temperatūru starojoši apgabali, kas pārklājas ar depresīvas koronālās emisijas apgabaliem, no kuriem nāk atvērtas magnētiskā lauka līnijas. Pētījumā izmantoti ar Nobejamas Radio Heliogrāfu NoRH (λ = 1.76 cm), Metsähovi Saules Observatorijas14-metrīgo radio teleskopu MRO-14 (λ = 0.8 cm) un Ventspils Starptautiskā Radio Astronomijas Centra 32-metrīgo radio teleskopu RT-32 (λ = 3.2 – 4.7 cm) iegūtie radioattēli. Lai samazinātu trokšņus ar RT-32 iegūtajās Saules radio kartēs, tika izmantota veiveleta "*à trous"* vienas plaknes telpiskā dekompozīcija, kas digitāli tika atņemta no katras kartes. Atvērtā magnētiskā lauka rajonu lokalizēšanai tika izmantota visas Saules koronālā magnētiskā lauka ar potenciālā lauka avota virsmas (PFSS) simulācija ar parametru R_{SS} =1.8 $R_{\odot}$. Secināts, ka atklātie maza mikroviļņu emisijas spožuma temperatūras apgabali atbilst tieviem koronālajiem caurumiem līdzīgiem apgabaliem (*dark lanes*) blakus aktīvajiem apgabaliem un rada augsni tālākiem Saules vēja pētījumiem.

08.02. 2017.